Received: 6 January 2022 | Revised: 7 May 2022 | Accepted: 12 May 2022

DOI: 10.1111/cas.15430

ORIGINAL ARTICLE

Cancer Science WILEY

RNA binding protein POP7 regulates ILF3 mRNA stability and expression to promote breast cancer progression

Yanni Huang[1,2] | Yizi Zheng[1,3] | Ling Yao[1,2] | Feng Qiao[4] | Yifeng Hou[1,2] | Xin Hu[1,2,4] | Daqiang Li[1,2,5] | Zhiming Shao[1,2,4]

[1]Department of Breast Surgery, Key Laboratory of Breast Cancer in Shanghai, Fudan University Shanghai Cancer Center, Fudan University, Shanghai, China

[2]Department of Oncology, Shanghai Medical College, Fudan University, Shanghai, China

[3]Department of Thyroid and Breast Surgery, Shenzhen Second People's Hospital/First Affiliated Hospital of Shenzhen University Health Science Center, Shenzhen, China

[4]Precision Cancer Medicine Center, Fudan University Shanghai Cancer Center, Shanghai, China

[5]Institutes of Biomedical Sciences, Fudan University, Shanghai, China

Correspondence
Zhiming Shao, Fudan University Shanghai Cancer Center, Fudan University, Shanghai, China.
Email: zhimingshao@yahoo.com

Funding information
This research was funded by the National Natural Science Foundation of China (NSFC), grant number 81874113.

Abstract

RNA binding proteins (RBPs) play pivotal roles in breast cancer (BC) development. As an RBP, Processing of precursor 7 (POP7) is one of the subunits of RNase P and RNase MRP, however, its exact function and mechanism in BC remain unknown. Here, we showed that expression of POP7 was frequently increased in BC cells and in primary breast tumors. Upregulated POP7 significantly promoted BC cell proliferation in vitro and primary tumor growth in vivo. POP7 also increased cell migration, invasion in vitro, and lung metastasis in vivo. Through RNA immunoprecipitation coupled with sequencing (RIP-seq), we found that POP7 bound preferentially to intron regions and POP7-binding peak associated genes were mainly enriched in cancer-related pathways. Furthermore, POP7 regulated Interleukin Enhancer Binding Factor 3 (ILF3) expression through influencing its mRNA stability. Knockdown of ILF3 significantly impaired the increased malignant potential of POP7-overexpressing cells, suggesting that POP7 enhances BC progression through regulating ILF3 expression. Collectively, our findings provide the first evidence for the important role of POP7 and its regulation of ILF3 in promoting BC progression.

KEYWORDS
breast cancer, ILF3, mRNA stability, POP7, RNA binding protein

1 | INTRODUCTION

RBPs interact with coding or noncoding RNAs, as well as some proteins, forming ribonucleoprotein complexes that regulate virtually all steps of RNA metabolism at the post-transcriptional level.[1–3] Given their diverse functions, it is unsurprising that dysregulated RBP expression leads to numerous human diseases including cancer.[4–7]

Breast cancer (BC) remains the most common diagnosed tumor in women all around the world. It has become clear that BC is a complex and heterogeneous disease.[8] Growing evidence shows that RBPs also play pivotal roles in breast tumorigenesis and development. For example, overexpression of HuR in BC cells inhibited tumor growth in mouse model through influencing tumor angiogenesis.[9] MCPIP1 could suppress breast tumor by destabilizing

Abbreviations: BC, Breast cancer; CCK-8, Cell counting kit-8; DFS, disease-free survival; FPKM, fragments per kilobase of transcript per million mapped reads; FUSCC, Fudan University Shanghai Cancer Center; HEK293T, Human embryonic kidney 293T; Hsp27, Heat shock protein 27; IHC, Immunohistochemistry; ILF3, Interleukin enhancer binding factor 3; KEGG, Kyoto Encyclopedia of Genes and Genomes; OS, overall survival; POP7, Processing of precursor 7; qPCR, Quantitative PCR; RBP, RNA binding protein; RFS, relapse-free survival; RIP, RNA immunoprecipitation; SE, standard error; SMN1, Survival motor neuron 1; TCGA, The Cancer Genome Atlas; TMA, Tissue microarray.

antiapoptotic genes transcripts.[10] RALY, TARBP2, FMRP, and many other RBPs have been reported to facilitate BC progression and metastasis.[11–13] Due to the variety of RBP-binding RNAs and the complexity of post-transcription regulation, a further understanding of RBPs in BC is desirable.

In a previous study,[14] we identified several RBPs related to BC tumorigenesis by performing a pooled in vivo CRISPR screening targeting 159 RBPs that were upregulated in BC cells, and POP7 was among the top-ranking RBPs (Figure S1). POP7 (Processing of Precursor 7) is a component of the Ribonuclease P (RNase P) complex and a component of Ribonuclease MRP (RNase MRP) as well. RNase P was initially discovered to be an endoribonuclease needed to process tRNA precursors.[15] It is composed of H1 RNA with catalytic activity and at least 10 protein subunits in human cells.[16] As for RNase MRP, its main function is cleavage of 5.8S rRNA precursors.[17,18] RNase MRP and RNase P are highly related as they share most protein subunits with each other, including POP7. Emerging roles of RNase P/MRP have been reported and most researches have focused on the catalytic RNA component or the complex as a whole.[19–21] But the exact role of these protein subunits individually remains unclear.[16,22]

POP7 has been found to have endogenous ATPase activity that might not be related to the primitive function of RNase P.[23] In addition, POP7 has been reported to interact with heat shock protein 27 (Hsp27) affecting RNase P holoenzyme activity[24] and it could interact with survival motor neuron 1 (SMN1), leading to the redistribution of POP7 into stress granules.[25] A recent study has shown POP7 could be a potential biomarker for prognosis of esophageal cancer.[26] However, the role of POP7 in BC has never been reported.

In this study, we aimed to elucidate the biological function and mechanism of POP7 in BC. We observed upregulated POP7 expression in BC and we demonstrated that POP7 promotes cell proliferation and migration in BC through cell functional experiments both in vitro and in vivo. The binding targets of POP7 were identified by RNA immunoprecipitation coupled with sequencing (RIP-seq) and ILF3 (Interleukin Enhancer Binding Factor 3) was verified as one of the targets. Moreover, POP7 could enhance BC development through regulating ILF3 mRNA stability and expression. Taken together, our findings implicated a pivotal new role for POP7 in BC progression through regulating expression of ILF3.

2 | MATERIAL AND METHODS

2.1 | Cell culture and reagents

Normal breast epithelial cell line MCF10A and HMEC, human embryonic kidney 293T (HEK293T) cell line and human BC cell lines were obtained from the Cell Bank of Type Culture Collection of Chinese Academy of Sciences (Shanghai, China). MCF10AT, DCIS, and CA1a cells were kindly provided by Professor Guohong Hu (University of Chinese Academy of Sciences, Shanghai, China). HMEC cells and MCF10 cell lines were cultured as previously described.[14] Other cell lines were cultured in high-glucose DMEM containing 10% FBS (Gibco) and 1% penicillin/streptomycin. Cell culture media and supplements were all from BasalMedia (Shanghai, China). Chemicals and reagents were from Sigma-Aldrich (MO, USA) unless noted. Actinomycin D was obtained from MedChemExpress (NJ, USA).

2.2 | Tissue samples

In total, 10 pairs of breast tumor tissues and matched adjacent noncancerous tissues and 185 primary BC specimens were obtained from BC patients who had undergone surgical operations at Fudan University Shanghai Cancer Center (FUSCC). The study was approved by the Institutional Review Board of FUSCC and was conducted in accordance with the Declaration of Helsinki. Written informed consent was received from all participants. All samples were confirmed by pathologic diagnosis and 185 tissue samples were used to generate a tissue microarray (TMA). The clinicopathological characteristics of this cohort is presented in Table S1.

2.3 | Plasmid construct, transfection, lentiviral production, and infection

Full length human POP7 cDNA was purchased from FulenGen (Guangzhou, China) and then subcloned into the expression vector pCDH-CMV-MCS-EF1-Puro (System Bioscience, USA) to generate pCDH-Flag-POP7. The primers used for molecular cloning are provided in Table S2. POP7 knockdown cells were generated using LentiCas9-Blast and LentiGuide-Puro vectors (Addgene, USA) using the CRISPR/Cas9 system as previously described.[27] The sgRNAs targeting POP7 were chose from the GeCKO library (http://www.addgene.org/) and cloned into the LentiGuide-Puro vector. Small interfering RNAs (siRNAs) targeting ILF3 and the negative control were obtained from GenePharma (Shanghai, China). The siRNA targeting sequences are provided in Table S3. Transient transfection of plasmids and siRNAs was carried out using Lipofectamine 2000 transfection reagent (Invitrogen, USA). To establish stable cell lines, lentivirus packaging plasmid mix, and expression vectors were co-transfected into HEK293T cells. At 48 h after transfection, the viral supernatant was collected and filtered. Target cells were then infected with the virus in the presence of polybrene (Sigma-Aldrich) and selected with 1–2 μg/mL puromycin for 3 days.

2.4 | Cell proliferation assays

For CCK-8 (Cell Counting Kit-8; Dojindo, Japan) assay, cells were seeded into 96-well plates (1000/2000 cells per well). Cell viability was determined by the absorbance at 450 nm after incubating with CCK-8 solution for 2 h. For colony formation assay, cells were plated onto 6-well plates (1000 cells per well for T47D/ Hs578T, 500 cells for others) in triplicate and were cultured under normal condition for 10–14 days. Colonies were fixed with methanol and stained

with 0.5% crystal violet. The colonies were then photographed and counted.

2.5 | Cell migration and invasion assays

For the wound-healing assay, cells were plated onto 6-well plates and then the wound was created by 200 μl tips when cells were grown to confluency. Floated cells were washed with PBS, and the culture medium was replaced by serum-free medium. Images of the wound were taken at the indicated time points, and the wound closure ratios were calculated from three independent replicates. For migration and invasion assays, Transwell chambers and Biocoat Matrigel invasion chambers (Corning, USA) were used, respectively. Cells in serum-free medium were seeded into the top chamber (2×10^4 cells for migration and 5×10^4 cells for invasion assays). Growth medium containing 10% FBS was placed in the lower chamber. After incubating for 18–24 h, cells were fixed with methanol and stained with 0.5% crystal violet. Migrated and invaded cells were photographed and counted under the microscope.

2.6 | Quantitative real-time PCR

Total RNAs were extracted using TRIzol reagent (Invitrogen, USA) and converted into cDNAs using the PrimeScript RT Master Mix (TaKaRa, Japan). Quantitative real-time PCR (qPCR) was undertaken using SYBR Premix Ex Taq (Tli RNase H Plus; Takara) following the manufacturer's protocol. The primers used for qPCR were synthesized at Synbio Technologies (Suzhou, China; Table S4). All results were normalized to GAPDH and presented as fold induction relative to the control.

2.7 | Immunohistochemistry (IHC) and evaluation

Immunohistochemistry staining was carried out as previously described.[28,29] The staining results were scored by two independent pathologists who were blinded to the clinicopathologic information. Slides were evaluated using light microscopy and scored semiquantitatively as described previously.[14] A sum index (SI) was calculated using the sum of the staining intensity (1, weak; 2, moderate; 3, strong) and percentage of stained cells (1, <10%; 2, 10 to < 50%; 3, 50–100%), and then it was scored as follows: SI = 2, scored as 0; =3, scored as 1; =4, scored as 2; =5 or 6, scored as 3. As the TMAs represented duplicate samples for each case, the subsequently analyzed score was the average of the two available scores. Tumors with a score of 2 or greater were considered to exhibit high POP7 expression.

2.8 | Animal models

For tumor formation, MDA-MB-231 cells stably expressing pCDH or Flag-POP7 (4×106 cells/mouse) were harvested and resuspended in 50 μl PBS and 50 μl Matrigel. Cells were injected into the mammary fat pad of 6-week-old female BALB/c nude mice. Tumors were measured once a week after formation, and tumor volumes were calculated using the formula (length × width2)/2. After 7 weeks of injection, xenograft tumors were harvested. For lung metastasis assay, MDA-MB-231 cells (2×106 cells in 100 μl PBS/mouse) were injected directly into the tail veins of 6-week-old female BALB/c nude mice. After 5 weeks of injection, the lungs were removed, and metastatic nodules were counted. Paraffin-embedded lung sections were stained with H&E to verify the presence of lung metastasis. All animal studies were approved by the Institutional Animal Care and Use Committee of FUSCC, and all animal care was in accordance with relevant institutional guidelines.

2.9 | Antibodies and immunoblotting analysis

The primary antibodies used in this study are listed in Table S5. The HRP-linked secondary antibodies were obtained from Cell Signaling Technology. Immunoblotting analysis was performed as previously described in detail.[29,30]

2.10 | RIP-Seq, RNA-Seq, and data analysis

RIP was performed as previously described in detail.[31,32] Anti-POP7 antibody was used to immunoprecipitate POP7–RNA complexes, with input as the control. POP7-bound RNAs were isolated using TRIzol and analyzed through qPCR assay or high-throughput sequencing. A cDNA library was constructed using the TruSeq RNA library preparation kit (Illumina) and then sequenced using the Illumina HiSeq X Ten platform by ABLife Inc. (Wuhan, China). Reads were aligned to the human reference genome (hg38) using TopHat2 software.[33] Peak calling was conducted using two algorithms: Piranha (http://smithlab.usc.edu) and ABLIRC.[32] Binding motif analysis was performed using HOMER software.[34] RNA sequencing (RNA-seq) was performed as described previously.[35] Briefly, the RNA-seq library was constructed using the VAHTS mRNA-seq Library Prep Kit (Vazyme Biotech, China), qualified by Agilent 2100, and sequenced using the Illumina HiSeq platform. For data processing, after pretreatment, raw reads were mapped against the hg38 genome using HISAT2.[36] Gene expression levels were determined by fragments per kilobase of transcript per million mapped reads (FPKM) values using the DESeq2 package.

2.11 | mRNA stability assays

MDA-MB-231 cells stably expressing pCDH or Flag-POP7 were treated with 5 μM Actinomycin D (Act D, MCE) to block new RNA synthesis for 0, 2 or 4, and their RNA was isolated using TRIzol and subsequently subjected to RNA-seq. For validation of RNA-seq results, relative transcript levels were assessed by qPCR, and 18S

rRNA was used as the normalization control. To detect the effect of POP7 on ILF3 mRNA stability, cells were treated with Act D and RNA was extracted and reverse transcribed for qPCR. The different fold changes of transcript levels between Flag-POP7 and pCDH cells were used as a measure of stability.

2.12 | Statistics

Statistical analyses were performed using SPSS 23 (IBM) or Prism 7 (GraphPad). All data are presented as mean ± standard error (SE) for triplicate experiments unless otherwise noted. For most experiments, an unpaired two-tailed Student *t*-test was utilized to compare the two groups of data. The Kaplan–Meier method and log-rank test were used for survival analysis. *p*-values less than 0.05 were considered statistically significant.

3 | RESULTS

3.1 | POP7 expression and prognosis in breast cancer and in public databases

We first explored the Oncomine Platform (https://www.oncomine.org) and found the mRNA levels of POP7 were upregulated in cancer compared with normal tissue in 44 data sets, including various types of cancer (Figure 1A). Specifically, in data sets of TCGA and Richardson Breast Statistics, POP7 showed a 1.622- and 1.688-fold increase ($p = 3.46E\text{-}41$; $p = 7.53E\text{-}5$) in breast tumor compared with in normal tissue, respectively (Figure 1B,C). In addition, data from UALCAN database[37] showed that POP7 expression also increased with a higher BC stage (Figure 1D).

The protein expression of POP7 was first validated in the MCF10 series of cell lines that have been described to offer a tumor progression model. Consistent with our earlier RNA-seq data,[14] immunoblotting showed that POP7 was indeed low in MCF10A cells, and higher in other MCF10 sublines (Figure 1E). We then examined its expression in normal MCF10A and HMEC cells and 11 commonly used BC cell lines and found that POP7 expression was higher in most BC cells (Figure 1F). Furthermore, immunoblotting was done using 10 pairs of patient breast tumor tissues and matched noncancerous tissues. Consistent with public databases, expression of POP7 was higher in tumor specimens in most samples (Figure 1G).

To explore the potential clinical significance of POP7, we found that high POP7 expression was correlated with worse overall survival (OS) and relapse-free survival (RFS) for BC patients using the KM plotter database (Figure 1H).[40] Immunohistochemistry staining was carried out using TMA, which included 185 samples of BC patients with clinical and follow-up information (Figure 1I). The clinicopathological characteristics of the cohort is presented in Table S1 and high POP7 expression was observed in 74.1% (137/185) of all patients. Kaplan–Meier analysis illustrated that patients with high POP7 expression appeared relatively worse survival (OS and disease-free survival, DFS), however, due to limited number of patients, the differences were not significant ($p = 0.438$ for OS and 0.099 for DFS; Figure 1J).

3.2 | POP7 promotes breast cancer cell proliferation and tumor growth in vivo

Based on POP7 expression in cell lines, we chose MCF7 and T47D cells to generate stable cell lines in which POP7 was knocked down, and MDA-MB-231 and Hs578T cells stabled expressed pCDH and Flag-tagged POP7 using lentiviral infection (Figure 2A–C). To examine the biological role of POP7, a series of functional assays was carried out using the above stable cells. Results of CCK-8 and colony formation assays showed that knockdown of POP7 impaired colony formation and cell proliferation of MCF7 and T47D cells (Figure 2D,F). In contrast, overexpression of POP7 promoted cell proliferation in MDA-MB-231 and Hs578T cells (Figure 2E,G). To determine whether POP7 could promote breast tumor growth in vivo, we injected MDA-MA-231 cells overexpressing POP7 or pCDH into the mammary fat pads of female BALB/c nude mice. Consistently, overexpression of POP7 accelerated tumor growth speed and tumor weights compared with the control group (Figure 2H–J). These results together suggested that POP7 enhanced BC cell proliferation and growth of tumor in vivo.

3.3 | POP7 promotes breast cancer cell migration, invasion, and tumor metastasis

To evaluate the effect of POP7 on the migratory and invasive capability of BC cells, migration, and invasion assays were carried out using MDA-MB-231 and Hs578T cells that stably expressed POP7. Wound-healing assay suggested that upregulated POP7 enhanced the rate of wound closure compared with the negative control (Figure 3A,B). In addition, the Transwell migration assay also showed high expression of POP7 increased the number of migrated cells (Figure 3C). The invasive capability of cancer cells was assessed using Matrigel invasion assay. Consistently, POP7 expression significantly enhanced the number of invaded cells through Matrigel-coated chambers (Figure 3D). In addition, to examine the role of POP7 on metastasis in vivo, we conducted tail vein injection in BALB/c nude mice using POP7-overexpressed MDA-MA-231 cells and their pCDH control. As shown in Figure 3E,F, there were more metastatic tumor nodules in the lungs in POP7 overexpressed cells. H&E staining confirmed the formation of metastatic nodules in the lungs (Figure 3G). Together, these results suggested that POP7 promotes the potential of migration and invasion of BC cell in vitro and tumor metastasis in vivo.

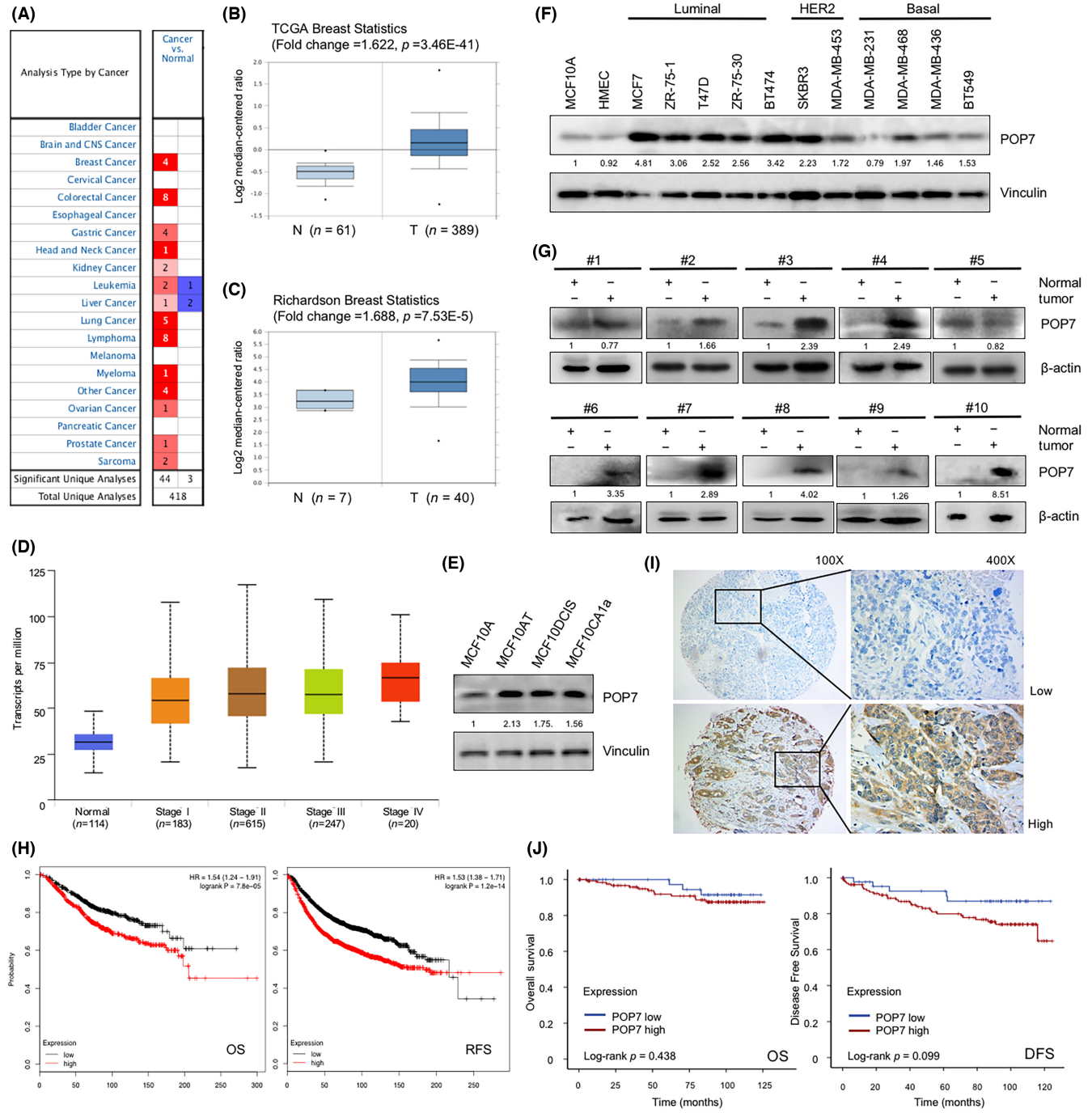

FIGURE 1 POP7 expression is upregulated in breast cancer and in public databases. (A–C) POP7 mRNA levels in the Oncomine database in all 418 data sets (A) and in data sets of breast statistics (B) and (C). (D) POP7 mRNA expression in different clinical stages of breast cancer in the UALCAN database. (E, F) Immunoblotting analysis of POP7 protein expression in MCF10 serial cell lines (E) and in 11 breast cancer cell lines and normal MCF10A and HMEC cells (F). (G) Immunoblotting analysis of POP7 protein expression in 10 pairs of matched breast cancer specimens and adjacent normal breast tissues. (H) Kaplan–Meir analysis of OS and RFS using the KM plotter database. (I) Representative images of the immunohistochemistry analysis of POP7 expression. (J) Kaplan–Meir analysis of OS and DFS using the FUSCC cohort. A log-rank test was used to determine the statistical significance between the POP7 low expression group ($n = 48$) and high expression group ($n = 137$)

3.4 | Identification and landscape of POP7 targeted binding RNAs by RIP-seq

As POP7 is one of the subunits of RNase MRP, we speculated whether POP7 could impact processing of pre-rRNAs. Therefore, we examined the expression of pre-rRNAs (including 45S, 28S, 18S, and 5.8S rRNA) using qPCR and found that POP7 did not influence their expression significantly (Figure S2). In addition, as POP7 is also a component of RNase P, considering various tRNAs, RIP-seq was chosen to investigate whether POP7 had an effect on

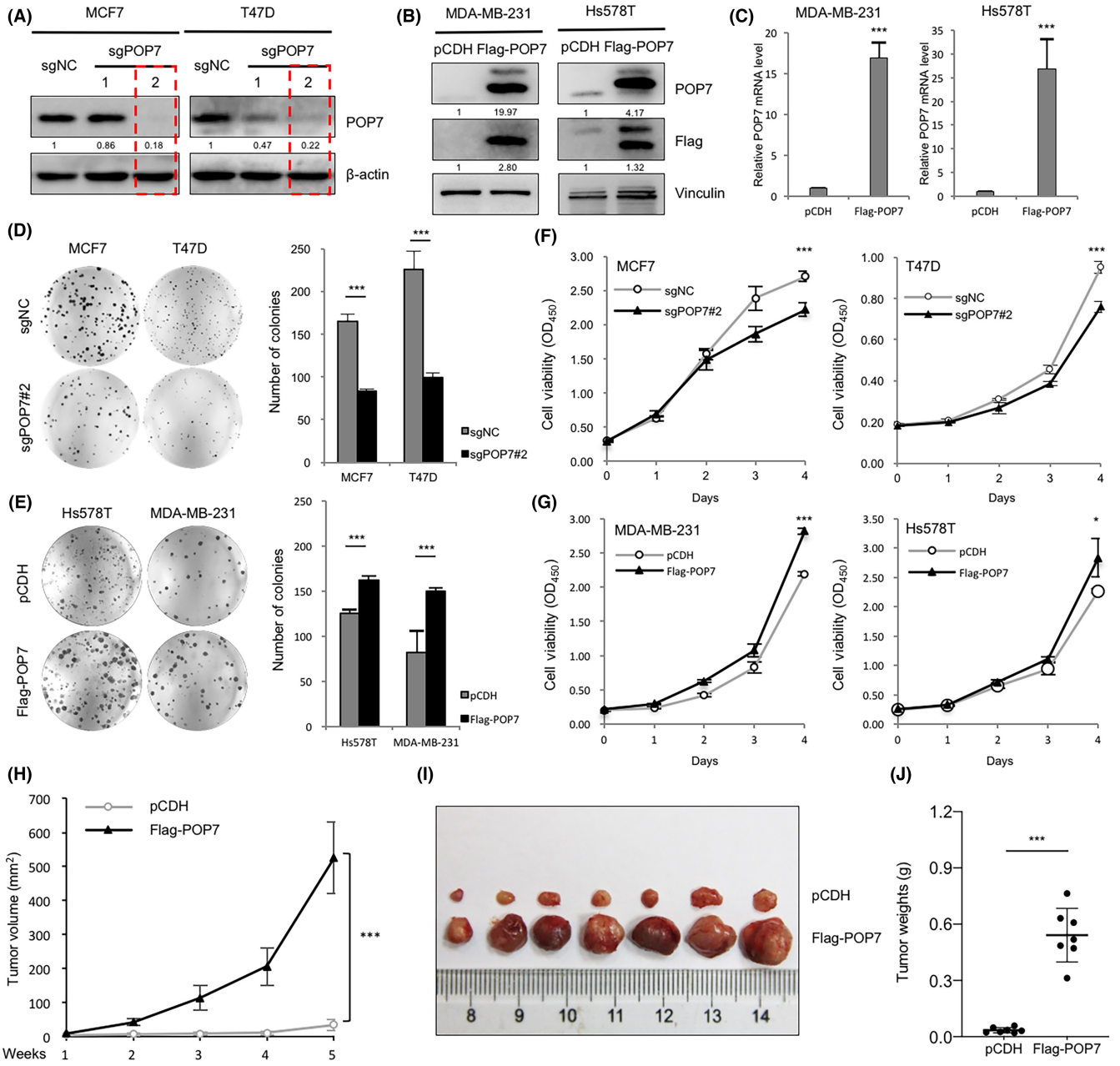

FIGURE 2 POP7 promotes breast cancer cell proliferation in vitro and tumor growth in vivo. (A) Immunoblotting analysis of CRISPR-mediated knockdown of POP7 in MCF7 and T47D cells. (B, C) MDA-MB-231 and Hs578T cells stably expressing pCDH and Flag-POP7 were subjected to immunoblotting (B) and qPCR (C) analysis of POP7 protein and mRNA levels, respectively. (D, E) The above cells were subjected to cell viability assays using colony formation. Representative images of survival colonies (left) and corresponding quantitative results (right) are shown. (F, G) The above cells were subjected to determination of cell viability using the CCK-8 assay. (H–J) MDA-MB-231 cells stably expressing pCDH and Flag-POP7 were injected into mammary fat pads of female BALB/c nude mice ($n = 7$). Xenograft tumor growth curves (H), photographs of harvested tumors (I), and tumor weights (J) are shown. Data are presented as mean ± SEM. $^{***}p < 0.001$, $^{**}p < 0.01$, $^{*}p < 0.05$

tRNA generation, and to identify POP7-associated target RNAs in a genome-wide range.

Immunoprecipitation of POP7-associated RNAs was carried out in MDA-MB-231 cells stably expressing Flag-POP7 and two biological replicates were performed with a correlation coefficient of 0.72 (Figure 4A). The cDNA libraries were sequenced and the distribution of uniquely mapped reads was categorized. Reads are mostly enriched in introns and intergenic regions and, compared with input, these reads are significantly higher in the immunoprecipitation (IP) sample (34.27% vs 25.99%; Figure 4B; Table S6). It is worth noting that reads are not enriched in regions of noncoding exons (nc_exon), which would change if POP7 could influence the generation and expression of tRNAs.

Peak calling was conducted and the distribution of specific peaks was categorized. Consistently, peaks were mainly enriched in the introns and intergenic regions (Figure 4C; Table S6). POP7-binding

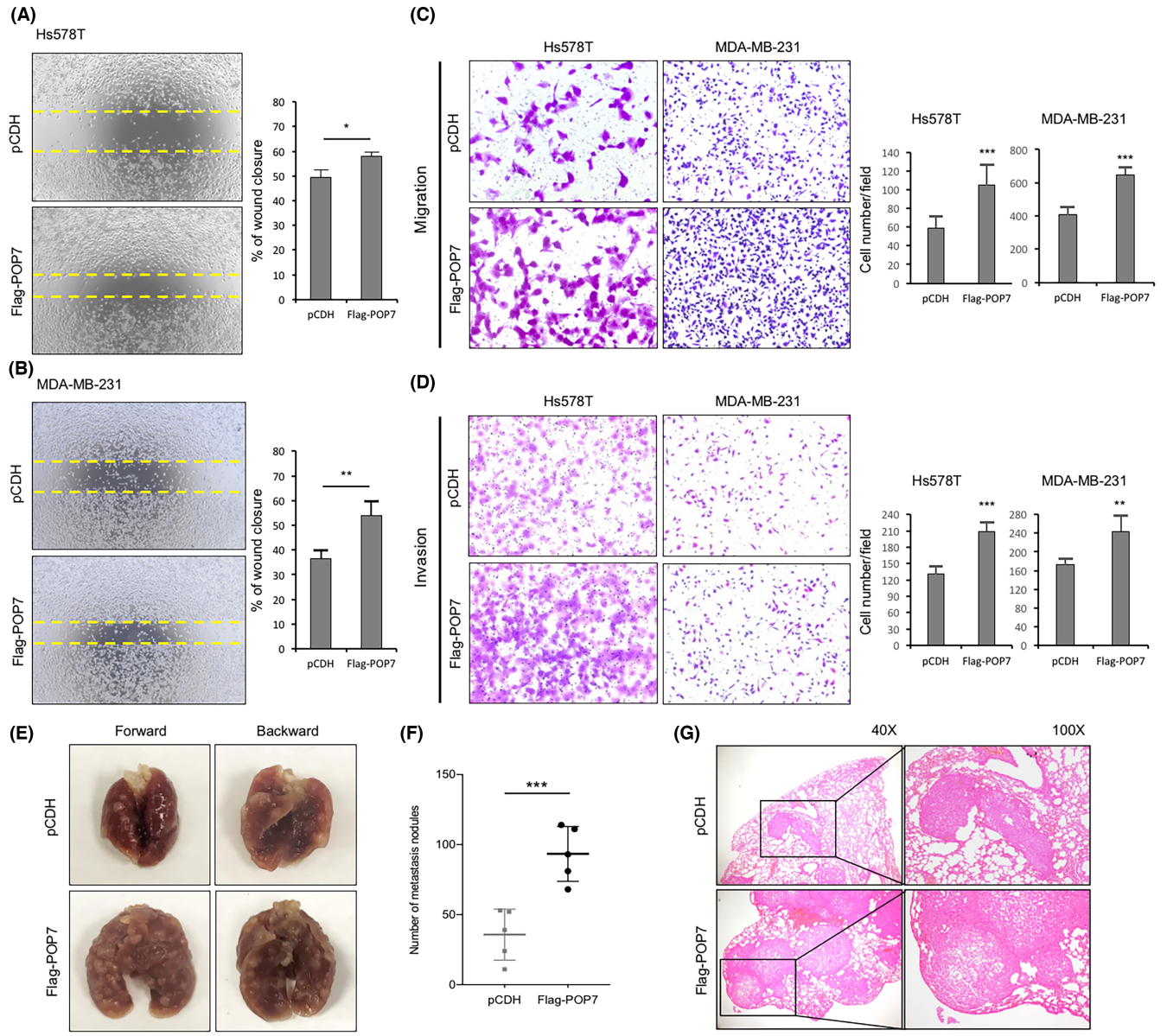

FIGURE 3 POP7 promotes breast cancer cell migration, invasion, and tumor metastasis. (A, B) Wound-healing assays were carried out using MDA-MB-231 and Hs578T cells stably expressing pCDH and Flag-POP7. Representative images (left) and corresponding quantitative results (right) are shown. (C, D) Transwell migration (C) and Matrigel invasion (D) assays were carried out using the resultant MDA-MB-231 and Hs578T cells. Representative images of cell migration and invasion (left) and quantitative results (right) are shown. (E–G), MDA-MB-231 cells stably expressing pCDH and Flag-POP7 were injected through the tail vein into BALB/c nude mice ($n = 5$). Representative photographs of metastatic lung nodules (E), quantitative results of nodules (F), and H&E staining sections of lung tissues (G) are shown. Data are presented as the mean ± SEM. $^{***}p < 0.001$, $^{**}p < 0.01$, $^{*}p < 0.05$

motifs were analyzed and the GGUAAG motif or GC-rich pattern was among the most enriched motifs (Figures 4D and S3). KEGG pathway analysis were conducted for peak associated genes and the top 10 enriched pathways are shown (Figure 4E). Focal adhesion, proteoglycans in cancer, and cancer-related pathways including PI3K-Akt pathway and Notch signaling pathway are among the top pathways.

We further analyzed the above results through overlapping peaks identified by two algorithms and by two replicates, respectively. Then we obtained 143 overlapped peaks and 90 corresponding genes as shown in the Venn diagram (Figure 4F; Table S7). KEGG analysis was also conducted for these 90 genes and results showed that pathways related to cancer, such as Focal adhesion, Notch, and Hippo signaling pathway, were also enriched (Figure 4G).

3.5 | POP7 regulates ILF3 expression through influencing its mRNA stability

RBPs are known to function through diverse molecular mechanisms,[7] regulation of mRNA stability is one of the most important

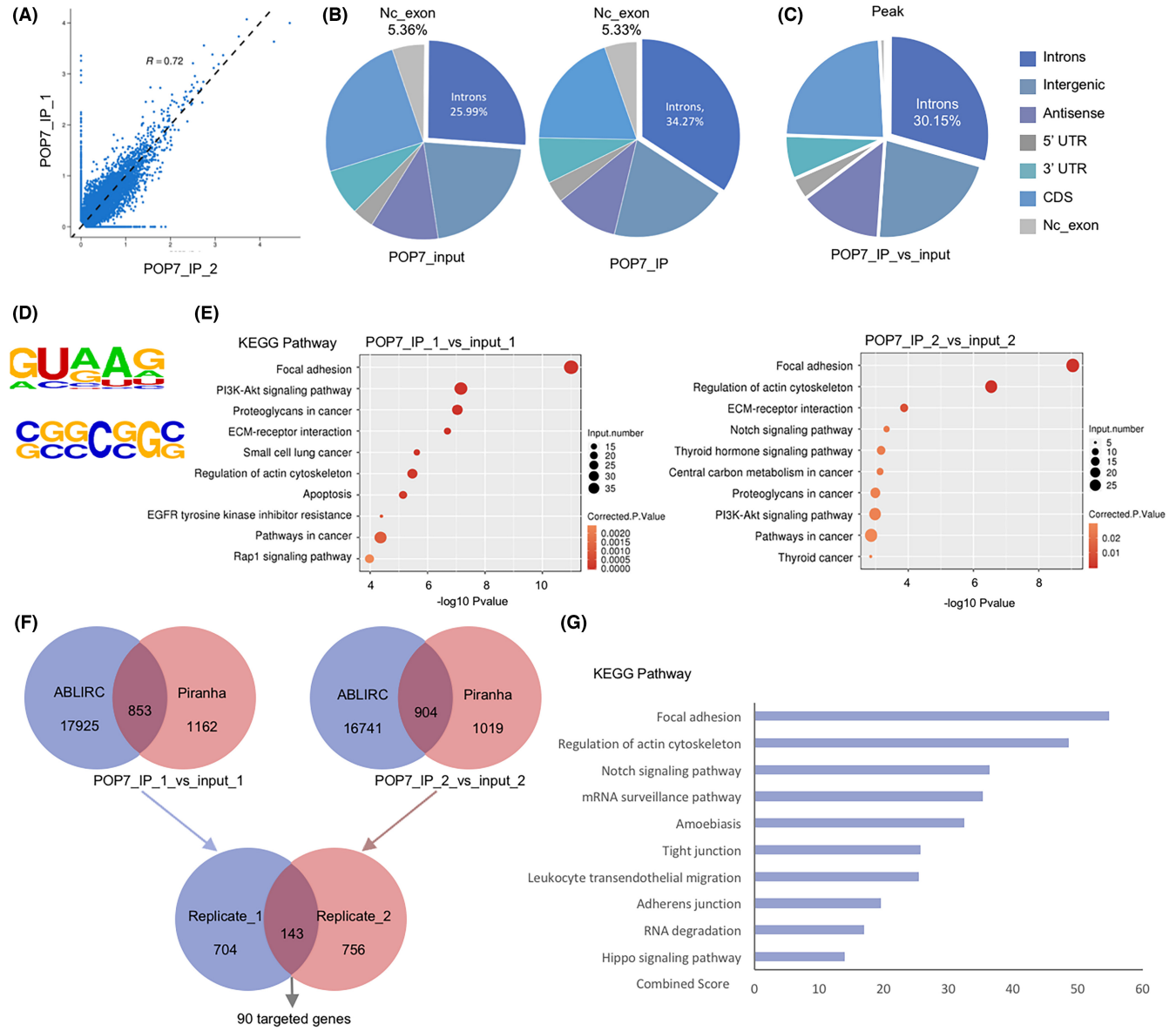

FIGURE 4 Identification and landscape of POP7 targeted binding RNAs by RIP-seq. (A) Scatterplot and correlation coefficients of the RIP-seq read counts between two biological replicates. (B) Pie charts of the distribution of uniquely mapped anti-POP7 reads across different genomic regions. (C) Pie chart of the distribution of POP7 RIP-seq peaks across different genomic regions. (D) Motif analysis identifying the most enriched binding motifs of POP7. (E) KEGG pathways of POP7-binding peak associated genes. (F) Venn diagrams of overlapping peaks bound by POP7 by two algorithms and by two replicates. (G) KEGG pathways of 90 overlapping peak associated genes

functions. According to the RIP-seq data, we supposed that POP7 could also affect the mRNA stability of its target RNAs. Therefore, we treated MDA-MB-231 cells (pCDH and POP7-overexpressed) with Act D for 0 h, 2 h, or 4 h and extracted RNAs were sent for RNA-seq. The mRNA expression levels of the above 90 overlapped genes were further analyzed to show the change across time. Compared with the control, upregulated POP7 expression indeed had different impacts on the stability of these target mRNAs (Figure 5A).

We picked genes that were significantly changed in mRNA stability for validation using qPCR (data not shown). Finally, Interleukin Enhancer Binding Factor (ILF3) was chosen as RIP-qPCR validated its interaction with POP7 (Figure 5B) and it was verified that overexpressed POP7 could enhance its mRNA stability and vice versa (Figure 5C). In addition, the mRNA level of ILF3 did not change significantly when POP7 expression was up/downregulated (Figure S4A,B). The Integrative Genomics Viewer (IGV) showed that binding peaks of POP7 are mainly localized in the 5′UTR region of ILF3 pre-mRNA, indicating there might be certain unknown elements responsible for the regulation of its mRNA stability (Figure S4C). Given that POP7 enhances ILF3 mRNA stability, it might therefore lead to elevated protein levels of ILF3. Knockdown of POP7 indeed decreased ILF3 protein expression, whereas overexpression of POP7 led to increased protein abundance of ILF3 (Figure 5D).

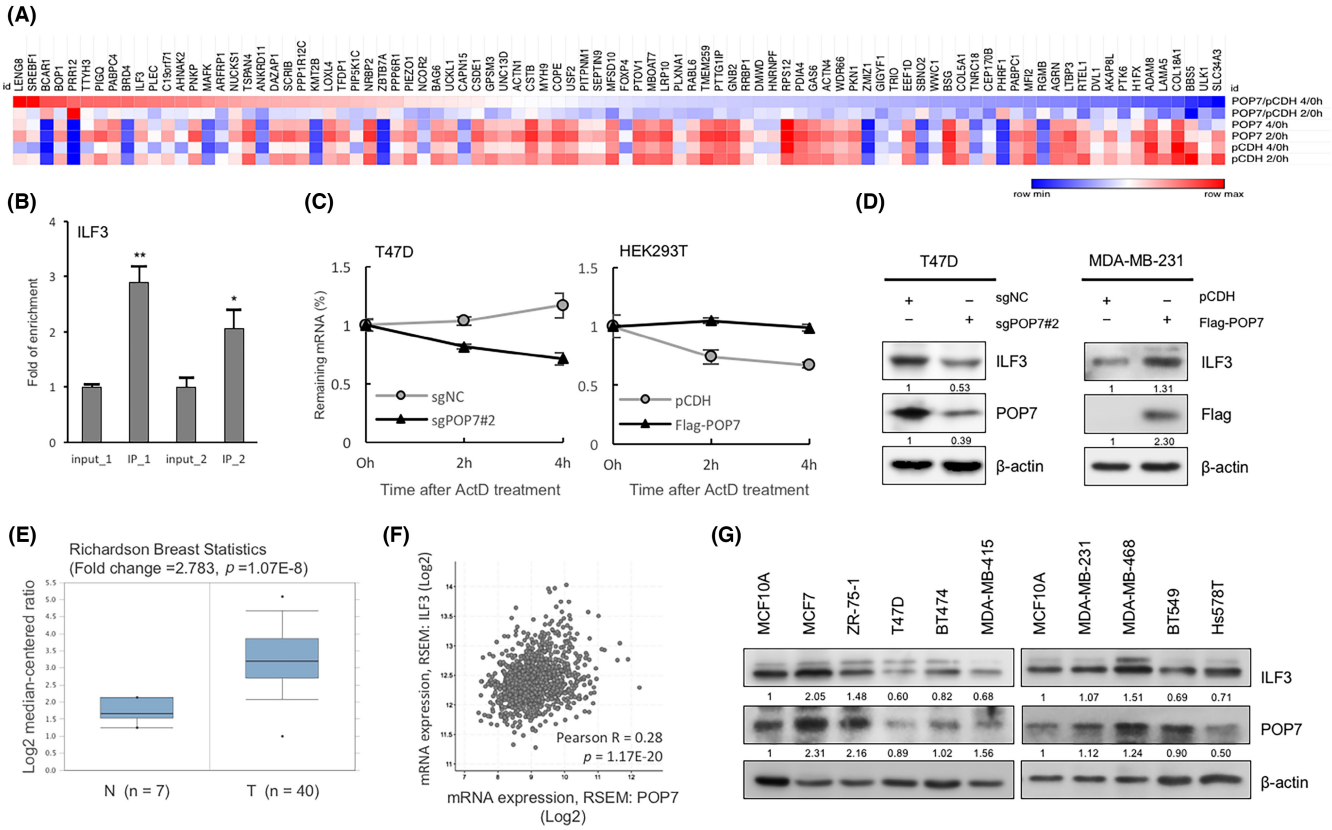

FIGURE 5 POP7 regulates ILF3 expression by influencing its mRNA stability. (A) Heatmap of the mRNA levels of the 90 overlapping peak associated genes after treatment with Act D for 0, 2, or 4 h in MDA-MB-231 pCDH or POP7 overexpressing cells. (B) RIP-qPCR validation of the POP7 binding with ILF3 in MDA-MB-231 cells. The peak of ILF3 that was common to both replicates was chosen for validation. Data are presented as mean ± SEM (**$p < 0.01$, *$p < 0.05$). (C) ILF3 mRNA stability assay in T47D and HEK293T cells by qPCR. The data were normalized and are represented as a percentage of the mRNA levels measured at time 0, before adding Act D. (D) Effects of POP7 expression on ILF3 protein level in T47D and MDA-MB-231 cells by immunoblotting analysis. (E) Analysis of ILF3 mRNA levels in the Oncomine database. (F) Analysis of the correlation between POP7 and ILF3 expression in TCGA database. (G) Immunoblotting analysis of POP7 and ILF3 proteins in breast cancer cell lines and normal MCF-10A cell line

ILF3 has been reported to be highly expressed in various cancers,[41–44] so we examined the Oncomine database and found that it showed increased mRNA expression in breast tumor (Figure 5E). The mRNA expression of POP7 was correlated with ILF3 in BC (Pearson R = 0.28, p = 1.17E-20) shown by TCGA data (Figure 5F).[45] The correlation between POP7 and ILF3 protein abundance was also observed in common BC cell lines using immunoblotting analysis (Figure 5G).

These results together indicated that POP7 could affect ILF3 expression through a post-transcriptional regulatory mechanism by influencing the mRNA stability of ILF3.

3.6 | POP7 enhances breast cancer progression through regulating ILF3 expression

Given that POP7 regulated mRNA stability and the subsequent abundance of ILF3, we attempted to verify ILF3 as a potential regulator of BC progression downstream of POP7. To confirm this, POP7-overexpressed MDA-MB-231 and Hs578T cells were transfected with siRNAs targeting ILF3 or negative control siNC (Figures 6A and S5A). Cell growth and colony formation assays indicated that knockdown of ILF3 by siRNA significantly impaired the proliferation capacity of POP7 overexpressed cells compared with the control (Figures 6B–D and S5B–D). Moreover, knockdown of ILF3 expression markedly restored POP7 overexpression-induced cell migratory and invasive capacities, revealed by the Transwell migration and Matrigel invasion assays (Figures 6E,F and S5E,F). Together, these results showed that POP7 overexpression-induced enhanced BC progression can be reversed by knockdown of ILF3, indicating that POP7 promotes BC, at least partially, through its regulation of ILF3.

4 | DISCUSSION

To better understand BC, intensive efforts have been undertaken and there is already ample evidence that dysregulated RBPs have significant impacts on tumorigenesis and cancer progression, including BC.[6,7,46–48] Many RBPs have been reported to be abnormally expressed in cancers and correlated with clinical prognosis.[48,49] In

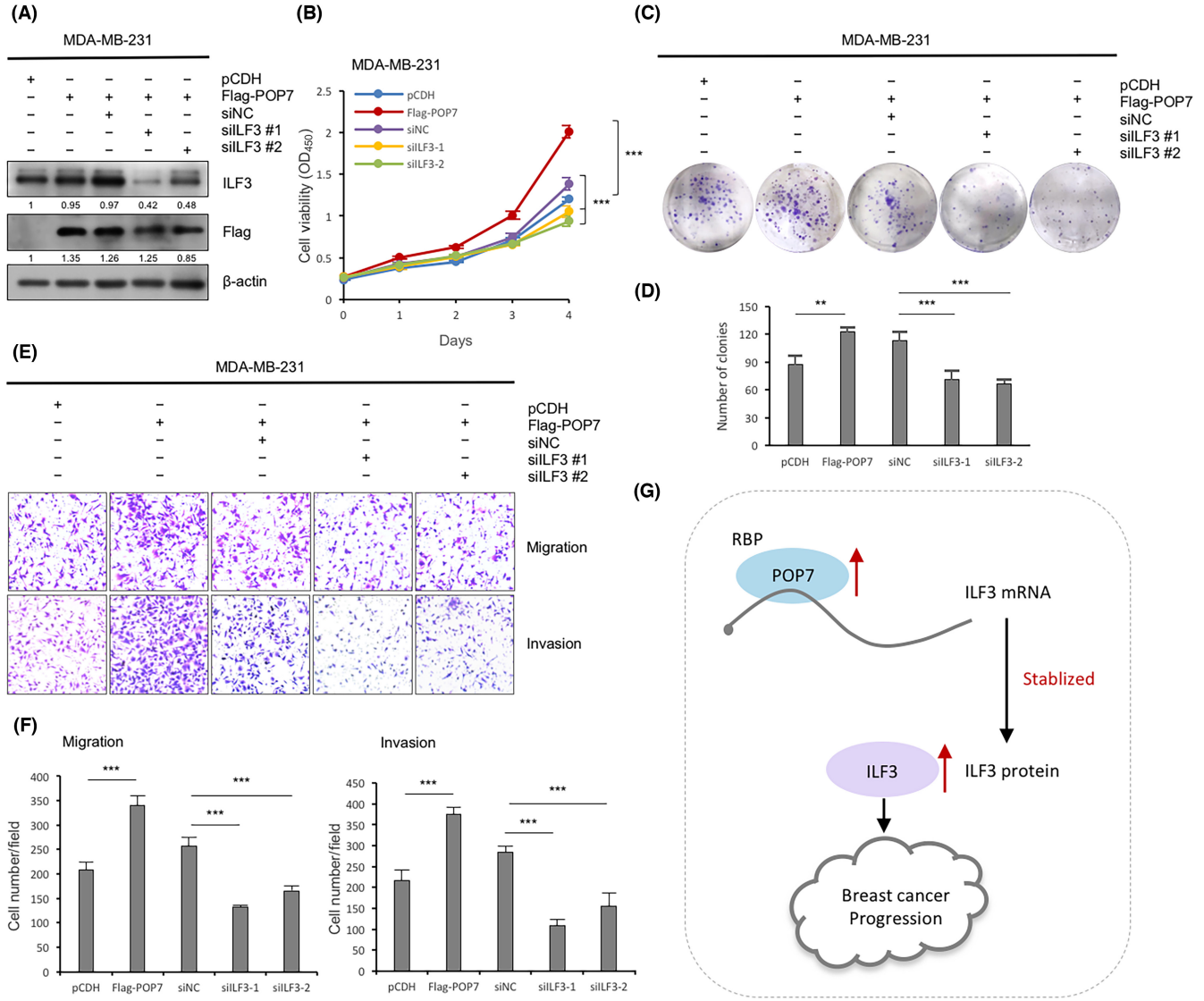

FIGURE 6 POP7 overexpression-induced enhanced breast cancer progression can be reversed by depletion of ILF3 expression. (A) MDA-MB-231 cells were transfected with two different siRNAs targeting ILF3 (siILF3#1/#2) or negative control siRNA (siNC). Cells were analyzed by immunoblotting after 48 h of transfection. (B–D) The transfected cells above were analyzed by CCK8 assays (B) and colony formation assays. Representative images (C) and quantitative results of colonies (D) are shown. (E, F) Transwell migration and Matrigel invasion assays were carried out using the resultant transfected MDA-MB-231 cells. Representative images of cell migration and invasion (E) and quantitative results (F) are shown. (G) The proposed working model of this study. Data are presented as mean ± SEM. $^{***}p < 0.001$, $^{**}p < 0.01$, $^{*}p < 0.05$

this study, by public database and immunoblotting, we found that expression of POP7 was upregulated in BC, suggesting that POP7 could potentially contribute to tumor malignancy. This result was also verified in BC cell lines using immunoblotting. IHC staining was performed and POP7 exhibited a high rate of positive expression, however high POP7 expression did not show a significant correlation with patients' worse prognosis. This may account for the limited number of patients and event rate in our study cohort. Therefore, a larger population study is still needed to confirm whether POP7 might be a prognostic marker for human BC.

Through binding to various different mRNAs, RBPs play central roles as oncoproteins or tumor-suppressor proteins.[46,49,50] To study the exact role of POP7 in BC, we performed a series of functional assays in vitro using POP7 knockdown or overexpressed cells. Our results suggested that POP7 could promote BC cell proliferation. Although there seems to be a discrepancy between in vitro and in vivo studies, the changes are statistically significant. As cell proliferation assays are relatively short term, whereas tumor growth in mice lasts for nearly a month, and due to the complex microenvironment in tumor tissues, a subtle distinction could lead to significant differences during tumor growth. We think that the combined effects of these factors resulted in the discrepancy. POP7 could facilitate BC migration and metastasis as well. By studies both in vitro and in vivo, we confirmed that POP7 plays an important role in BC progression. To the best of our knowledge, our study is the first report on POP7 involvement in BC progression.

Here, RIP-seq was first used to globally determine the landscape of POP7-associated RNAs in human cancer cells. We found that POP7 binds preferentially to intron regions of target RNAs. However, reads of POP7-associated RNAs were not enriched in the nc-exon region, where various noncoding RNAs including tRNAs are generated. Given that POP7 also had no significant impact on rRNA expression through qPCR results, we considered that POP7 might play its role in cancer not closely related to the function of RNase P/MRP. KEGG pathway analysis indicated that POP7-binding peak associated genes were relevant to cancer-related pathways, such as the Notch and Hippo signaling pathways, indicating that POP7 may have profound roles in regulating these cancer-related processes.

Regulation of mRNA stability is crucial for gene expression and is one of the main mechanisms through which RBPs mediate their multiple functions.[7,48,51,52] The AU-rich element (ARE) in the 3′UTR is the most common and the most studied structure regulating mRNA stability. RBPs such as HuR could bind to ARE-containing targets encoding important genes in carcinogenesis such as oncogenes, cell-cycle genes, and many other regulators.[53,54] In addition to AREs, there are other regulatory elements described to affect mRNA stability, such as constitutive decay element located downstream of the ARE.[55] All these elements cooperate with each other to achieve complex and dynamic control over mRNA stability. Our RNA-seq data supported this idea, as POP7 indeed showed different effects on the stability of its target RNAs. However, according to our RIP-seq, POP7 binds preferentially to intron regions of its targets. So we speculated that there might be other unknown elements responsible for the regulation of mRNA stability by POP7. This result is interesting and worthwhile to be further studied in the future.

Our research data validated that ILF3 might be an important target of POP7. Supporting this speculation, knockdown of POP7 significantly decreased ILF3 mRNA stability and vice versa. Although there was no significant change in ILF3 mRNA level, POP7 did alter the protein expression of ILF3, demonstrating that POP7 could regulate ILF3 expression through influencing its mRNA stability in BC. ILF3 has been observed overexpressed in many types of cancer, indicating its role in oncogenesis.[41–44,56] A previous study reported that ILF3 could increase vascular endothelial growth factor (VEGF) mRNA stability and protein expression under hypoxia conditions, facilitating breast tumor angiogenesis.[57] ILF3 could also facilitate tumor invasion by forming a complex with SMARCE1, influencing protease secretion to degrade the basement membrane.[58] Our research showed that ILF3 was upregulated in cancer and was correlated with POP7 expression. Moreover, knockdown of ILF3 expression by siRNA could significantly restore POP7-induced enhanced BC cell proliferation and migration. Therefore, our study results led us to propose a mechanism in which POP7 enhances BC progression through regulation of ILF3 expression (Figure 6G). It should be noted that our RIP-seq data showed that POP7-binding peaks were mainly localized in the 5′UTR region of ILF3 pre-mRNA. However, the potential role of the 5′UTR on mRNA stability remains elusive. A recent study has suggested that there are certain sequence features of the 5′UTR that are involved in the complex mRNA-surveillance pathways.[59] Further investigations, therefore, are still required to understand how POP7 affects the mRNA stability of ILF3 precisely.

In conclusion, our study reported a novel biological function of RNA binding protein POP7 in breast cancer-related pathological processes. And we reported for the first time the landscape of the genome-wide POP7-RNA interactions in BC cells using RIP-seq approach. ILF3 was identified as one of the POP7-binding transcripts that are directly regulated by POP7. Regulation of ILF3 expression and mRNA stability is through which, POP7 exerts its function on promoting BC. Our findings therefore provides new proof that POP7 could be implicated in BC development through regulation of ILF3, which will be helpful for discovering new clues for antitumor therapy of breast cancer in the future.

ACKNOWLEDGMENTS

We sincerely thank members in the Li laboratory for their technical assistance and helpful advice.

DISCLOSURE

The authors have no conflict of interest.

DATA AVAILABILITY STATEMENT

The data supporting the findings of this study are available from the corresponding author on reasonable request.

ETHICAL APPROVAL

All experimental protocols were approved by the Institutional Review Board of Fudan University Shanghai Cancer Center and performed in accordance with the relevant guidelines and regulations. Written informed consents were obtained from all patients. All animal experiments were approved by the Institutional Animal Care and Use Committee of FUSCC, and all animal procedures were in accordance with relevant institutional and national guidelines.

ORCID

Xin Hu https://orcid.org/0000-0002-8915-3526
Daqiang Li https://orcid.org/0000-0002-5113-2332
Zhiming Shao https://orcid.org/0000-0001-8781-2455

REFERENCES

1. Glisovic T, Bachorik JL, Yong J, Dreyfuss G. RNA-binding proteins and post-transcriptional gene regulation. *FEBS Lett*. 2008;582(14):1977-1986.
2. Gerstberger S, Hafner M, Tuschl T. A census of human RNA-binding proteins. *Nat Rev Genet*. 2014;15(12):829-845.
3. Hentze MW, Castello A, Schwarzl T, Preiss T. A brave new world of RNA-binding proteins. *Nat Rev Mol Cell Biol*. 2018;19(5):327-341.
4. Lukong KE, Chang KW, Khandjian EW, Richard S. RNA-binding proteins in human genetic disease. *Trends in genetics : TIG*. 2008;24(8):416-425.
5. Castello A, Fischer B, Hentze MW, Preiss T. RNA-binding proteins in Mendelian disease. *Trends in genetics : TIG*. 2013;29(5):318-327.
6. Calabretta S, Richard S. Emerging roles of disordered sequences in RNA-binding proteins. *Trends Biochem Sci*. 2015;40(11):662-672.

7. Pereira B, Billaud M, Almeida R. RNA-binding proteins in cancer: old players and new actors. *Trends in Cancer*. 2017;3(7):506-528.
8. Polyak K. Heterogeneity in breast cancer. *J Clin Invest*. 2011;121(10):3786-3788.
9. Gubin MM, Calaluce R, Davis JW, et al. Overexpression of the RNA binding protein HuR impairs tumor growth in triple negative breast cancer associated with deficient angiogenesis. *Cell Cycle (Georgetown, Tex)*. 2010;9(16):3337-3346.
10. Lu W, Ning H, Gu L, et al. MCPIP1 Selectively Destabilizes Transcripts Associated with an Antiapoptotic Gene Expression Program in Breast Cancer Cells That Can Elicit Complete Tumor Regression. *Cancer Res*. 2016;76(6):1429-1440.
11. Lucá R, Averna M, Zalfa F, et al. The Fragile X Protein binds mRNAs involved in cancer progression and modulates metastasis formation. *EMBO Mol Med*. 2013;5(10):1523-1536.
12. Goodarzi H, Zhang S, Buss CG, Fish L, Tavazoie S, Tavazoie SF. Metastasis-suppressor transcript destabilization through TARBP2 binding of mRNA hairpins. *Nature*. 2014;513(7517):256-260.
13. Bondy-Chorney E, Baldwin RM, Didillon A, Chabot B, Jasmin BJ, Cote J. RNA binding protein RALY promotes Protein Arginine Methyltransferase 1 alternatively spliced isoform v2 relative expression and metastatic potential in breast cancer cells. *Int J Biochem Cell Biol*. 2017;91(Pt B):124-135.
14. Zheng YZ, Xue MZ, Shen HJ, et al. PHF5A epigenetically inhibits apoptosis to promote breast cancer progression. *Cancer Res*. 2018;78(12):3190-3206.
15. Jarrous N, Altman S. Human ribonuclease P. *Methods Enzymol*. 2001;342:93-100.
16. Jarrous N, Gopalan V. Archaeal/eukaryal RNase P: subunits, functions and RNA diversification. *Nucleic Acids Res*. 2010;38(22):7885-7894.
17. Chang DD, Clayton DA. A mammalian mitochondrial RNA processing activity contains nucleus-encoded RNA. *Science (New York, NY)*. 1987;235(4793):1178-1184.
18. Walker SC, Aspinall TV, Gordon JM, Avis JM. Probing the structure of Saccharomyces cerevisiae RNase MRP. *Biochem Soc Trans*. 2005;33(Pt 3):479-481.
19. Thiel CT, Rauch A. The molecular basis of the cartilage-hair hypoplasia-anauxetic dysplasia spectrum. *Best Pract Res Clin Endocrinol Metab*. 2011;25(1):131-142.
20. Klemm BP, Wu N, Chen Y, et al. The Diversity of Ribonuclease P: Protein and RNA Catalysts with Analogous Biological Functions. *Biomolecules*. 2016;6(2):27.
21. Jarrous N. Roles of RNase P and its subunits. *Trends Genet*. 2017;33(9):594-603.
22. Gopalan V, Jarrous N, Krasilnikov AS. Chance and necessity in the evolution of RNase P. *RNA (New York, NY)*. 2018;24(1):1-5.
23. Li Y, Altman S. A subunit of human nuclear RNase P has ATPase activity. *Proc Natl Acad Sci U S A*. 2001;98(2):441-444.
24. Jiang T, Altman S. Protein-protein interactions with subunits of human nuclear RNase P. *Proc Natl Acad Sci U S A*. 2001;98(3):920-925.
25. Hua Y, Zhou J. Rpp20 interacts with SMN and is re-distributed into SMN granules in response to stress. *Biochem Biophys Res Commun*. 2004;314(1):268-276.
26. Yang X, Han B, He Z, et al. RNA-binding proteins CLK1 and POP7 as biomarkers for diagnosis and prognosis of esophageal squamous cell carcinoma. *Front Dev Biol*. 2021;9:715027.
27. Ran FA, Hsu PD, Wright J, Agarwala V, Scott DA, Zhang F. Genome engineering using the CRISPR-Cas9 system. *Nat Protoc*. 2013;8(11):2281-2308.
28. Liu HY, Liu YY, Yang F, et al. Acetylation of MORC2 by NAT10 regulates cell-cycle checkpoint control and resistance to DNA-damaging chemotherapy and radiotherapy in breast cancer. *Nucleic Acids Res*. 2020;48(7):3638-3656.
29. Sun R, Xie HY, Qian JX, et al. FBXO22 possesses both protumorigenic and antimetastatic roles in breast cancer progression. *Cancer Res*. 2018;78(18):5274-5286.
30. Zhang FL, Cao JL, Xie HY, et al. Cancer-associated MORC2-Mutant M276I regulates an hnRNPM-mediated CD44 splicing switch to promote invasion and metastasis in triple-negative breast cancer. *Cancer Res*. 2018;78(20):5780-5792.
31. Li W, Zhang Z, Liu X, et al. The FOXN3-NEAT1-SIN3A repressor complex promotes progression of hormonally responsive breast cancer. *J Clin Invest*. 2017;127(9):3421-3440.
32. Xia H, Chen D, Wu Q, et al. CELF1 preferentially binds to exon-intron boundary and regulates alternative splicing in HeLa cells. *Biochimica et biophysica acta Gene regulatory mechanisms*. 2017;1860(9):911-921.
33. Kim D, Pertea G, Trapnell C, Pimentel H, Kelley R, Salzberg SL. TopHat2: accurate alignment of transcriptomes in the presence of insertions, deletions and gene fusions. *Genome Biol*. 2013;14(4):R36.
34. Heinz S, Benner C, Spann N, et al. Simple combinations of lineage-determining transcription factors prime cis-regulatory elements required for macrophage and B cell identities. *Mol Cell*. 2010;38(4):576-589.
35. Yang LF, Yang F, Zhang FL, et al. Discrete functional and mechanistic roles of chromodomain Y-like 2 (CDYL2) transcript variants in breast cancer growth and metastasis. *Theranostics*. 2020;10(12):5242-5258.
36. Kim D, Langmead B, Salzberg SL. HISAT: a fast spliced aligner with low memory requirements. *Nat Methods*. 2015;12(4):357-360.
37. Chandrashekar DS, Bashel B, Balasubramanya SAH, et al. UALCAN: a portal for facilitating tumor subgroup gene expression and survival analyses. *Neoplasia*. 2017;19(8):649-658.
38. Soule HD, Maloney TM, Wolman SR, et al. Isolation and characterization of a spontaneously immortalized human breast epithelial cell line, MCF-10. *Cancer Res*. 1990;50(18):6075-6086.
39. Hu M, Yao J, Carroll DK, et al. Regulation of in situ to invasive breast carcinoma transition. *Cancer Cell*. 2008;13(5):394-406.
40. Nagy Á, Lánczky A, Menyhárt O, Győrffy B. Validation of miRNA prognostic power in hepatocellular carcinoma using expression data of independent datasets. *Sci Rep*. 2018;8(1):9227.
41. Jiang W, Huang H, Ding L, et al. Regulation of cell cycle of hepatocellular carcinoma by NF90 through modulation of cyclin E1 mRNA stability. *Oncogene*. 2015;34(34):4460-4470.
42. Cheng C-C, Chou K-F, Wu C-W, et al. EGFR-mediated interleukin enhancer-binding factor 3 contributes to formation and survival of cancer stem-like tumorspheres as a therapeutic target against EGFR-positive non-small cell lung cancer. *Lung Cancer*. 2018;116:80-89.
43. Shamanna RA, Hoque M, Pe'ery T, Mathews MB. Induction of p53, p21 and apoptosis by silencing the NF90/NF45 complex in human papilloma virus-transformed cervical carcinoma cells. *Oncogene*. 2013;32(43):5176-5185.
44. Hu Q, Lu YY, Noh H, et al. Interleukin enhancer-binding factor 3 promotes breast tumor progression by regulating sustained urokinase-type plasminogen activator expression. *Oncogene*. 2012;32(34):3933-3943.
45. Cerami E, Gao J, Dogrusoz U, et al. The cBio cancer genomics portal: an open platform for exploring multidimensional cancer genomics data. *Cancer Discov*. 2012;2(5):401-404.
46. Mohibi S, Chen X, Zhang J. Cancer the 'RBP' eutics–RNA-binding proteins as therapeutic targets for cancer. *Pharmacol Ther*. 2019;203:107390.
47. Moore S, Jarvelin AI, Davis I, Bond GL, Castello A. Expanding horizons: new roles for non-canonical RNA-binding proteins in cancer. *Curr Opin Genet Dev*. 2018;48:112-120.
48. Qin H, Ni H, Liu Y, et al. RNA-binding proteins in tumor progression. *J Hematol Oncol*. 2020;13(1):90.

49. Kang D, Lee Y, Lee J-S. RNA-binding proteins in cancer: functional and therapeutic perspectives. *Cancer*. 2020;12(9):2699.
50. Saini Y, Chen J, Patial S. The tristetraprolin family of RNA-binding proteins in cancer: progress and future prospects. *Cancers (Basel)*. 2020;12(6):1539.
51. Dang H, Takai A, Forgues M, et al. Oncogenic activation of the RNA binding protein NELFE and MYC signaling in hepatocellular carcinoma. *Cancer Cell*. 2017;32(1):101-114.e108.
52. Zhao L, Wang W, Huang S, et al. The RNA binding protein SORBS2 suppresses metastatic colonization of ovarian cancer by stabilizing tumor-suppressive immunomodulatory transcripts. *Genome Biol*. 2018;19(1):35.
53. Wang J, Guo Y, Chu H, Guan Y, Bi J, Wang B. Multiple functions of the RNA-binding protein HuR in cancer progression, treatment responses and prognosis. *Int J Mol Sci*. 2013;14(5):10015-10041.
54. Huang H, Weng H, Sun W, et al. Recognition of RNA N(6)-methyladenosine by IGF2BP proteins enhances mRNA stability and translation. *Nat Cell Biol*. 2018;20(3):285-295.
55. Stoecklin G, Anderson P. Posttranscriptional mechanisms regulating the inflammatory response. *Adv Immunol*. 2006;89:1-37.
56. Zhang W, Xiong Z, Wei T, et al. Nuclear factor 90 promotes angiogenesis by regulating HIF-1α/VEGF-A expression through the PI3K/Akt signaling pathway in human cervical cancer. *Cell Death Dis*. 2018;9(3):276.
57. Vumbaca F, Phoenix KN, Rodriguez-Pinto D, Han DK, Claffey KP. Double-stranded RNA-binding protein regulates vascular endothelial growth factor mRNA stability, translation, and breast cancer angiogenesis. *Mol Cell Biol*. 2007;28(2):772-783.
58. Sokol ES, Feng Y-X, Jin DX, et al. SMARCE1 is required for the invasive progression of in situ cancers. *Proc Natl Acad Sci*. 2017;114(16):4153-4158.
59. Jia L, Mao Y, Ji Q, Dersh D, Yewdell JW, Qian SB. Decoding mRNA translatability and stability from the 5′UTR. *Nat Struct Mol Biol*. 2020;27(9):814-821.

SUPPORTING INFORMATION

Additional supporting information can be found online in the Supporting Information section at the end of this article.

How to cite this article: Huang Y, Zheng Y, Yao L, et al. RNA binding protein POP7 regulates ILF3 mRNA stability and expression to promote breast cancer progression. *Cancer Sci*. 2022;113:3801-3813. doi: 10.1111/cas.15430